Evidence of Mixed Oxide Formation on the Cu/SiO 2 Interface

Article *in* The Journal of Physical Chemistry C · August 2017
DOI: 10.1021/acs.jpcc.7b06563

2 authors:

Noelia Benito
University of Concepción
16 PUBLICATIONS **120** CITATIONS
SEE PROFILE

Marcos Flores
University of Chile
43 PUBLICATIONS **219** CITATIONS
SEE PROFILE

THE JOURNAL OF PHYSICAL CHEMISTRY C

Article

pubs.acs.org/JPCC

Evidence of Mixed Oxide Formation on the Cu/SiO_2 Interface

Noelia Benito* and Marcos Flores

Departamento de Física, Facultad de Ciencias Físicas y Matemáticas, Universidad de Chile, Blanco Encalada 2008, Santiago de Chile, Chile

Supporting Information

ABSTRACT: The deposition of Cu onto SiO_2 has been carried out by electron beam evaporation in order to study the interface formation by X-ray photoelectron spectroscopy and angle resolved X-ray photoelectron spectroscopy. Shifts in the binding energy of Cu $2p_{3/2}$ and Si 2p bands, as well as in the Cu LMM kinetic energy, have been observed during the growth. These changes are indicative of a modification in the coordination number of Cu or the formation of M−O−M′ cross-linking bonds at the interface. Moreover, different coordination states of Cu^+ and Cu^{2+} (tetrahedral and octahedral) have been detected. Apart from different coordination numbers, a new chemical state appears during the Cu/SiO_2 interface formation. This new contribution, Cu^{x+}, is attributed to the formation of a mixed oxide Cu-O-Si. Additionally, two different stages of growth of the Cu/SiO_2 interface have been observed: The first one, where no metallic Cu is detected and a mixture of copper oxides is measured onto the SiO_2 substrate, and the second one, in which metallic Cu appears on the surface and a multilayer Cu^0/Cu^{x+}/Cu oxides/SiO_2 can be inferred.

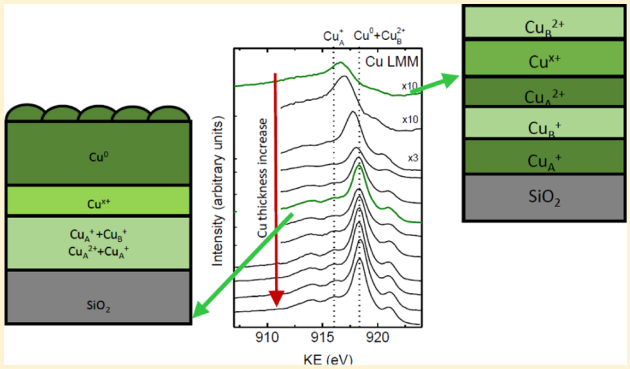

INTRODUCTION

With the development of ultra-large-scale integration (ULSI) devices, Cu has replaced Al as interconnection material due to its lower electrical resistivity (1.78×10^{-8} Ω m at 293 K) and its higher melting point (1357.6 K).[1] These properties make Cu more resistant to corrosion and to electromigration. However, Cu diffuses rapidly in Si[2] and SiO_2,[3] which causes degradation of electronic devices at relatively low temperature. During the last decades, a great effort has been done not only to find a suitable interdiffusion barrier material but also for the development of fabrication processes.[4−11] Several groups are studying self-forming barriers, fabricated by direct deposition of Cu−metal alloys or partially oxidized manganese onto the SiO_2 which form silicates that act as an effective Cu diffusion barrier.[12−15]

Moreover, the continuous downscaling of complementary metal oxide semiconductor (CMOS) devices and interconnections is limited by the need of layers thick enough to be continuous so as to provide robust performance. In this sense, several groups are working in the study of copper penetration into low-*k* dielectrics such as SiCOH or doped Si.[16,17] Most of them are interested in the failure of SiO_2 as an insulating dielectric due to the penetration of Cu by measuring time dependent dielectric breakdowns, *I*−*V* curves, or *C*−*V* curves, although several works report on Cu^+ diffusion by XPS.[18,19] Nevertheless, only a few publications are centered in understanding the problem of interface diffusion.

In this context, some theoretical calculations using molecular dynamic simulations of the Cu/Si interface formation have been carried out,[20,21] as well as the study of the initial stages of Cu/Si interface formation by AFM, STM, TEM, XRD, and RBS, even including the native oxide influence.[21−25] Otherwise, the Cu/SiO_2 interface, which is the base of the Cu/SiO_2/Si formation, has not been studied in depth. Espinós et al. studied the interfacial formation of Cu, CuO, and Cu_2O deposited on SiO_2, observing changes in the modified Auger parameter α' as the thickness of the Cu layer increases.[26] The authors attributed the change of this parameter to a modification in the coordination number of Cu, which causes a change in the Madelung potential around the photoemitting element and a subsequent variation of the BE and α' values. Another possibility is the formation of bonding interactions at the interface, due to the formation of M−O−M′ cross-linking bonds at the interface, where the bridging oxide ions should have different electronic characteristics than in the bulk oxides.[26]

This problem attracts the attention of the scientific community not only because this kind of system is needed in electronic devices but also because of the potential applications of the Cu/SiO_2 system in catalysis.[27,28] The surface and interface phenomena that occur are determined by the metal−support interactions,[29] which are more intense in catalytic systems formed by Cu nanoparticles on a flat SiO_2 substrate.[29,30] These systems have been studied from a

Received: July 4, 2017
Revised: August 10, 2017
Published: August 11, 2017

DOI: 10.1021/acs.jpcc.7b06563
J. Phys. Chem. C 2017, 121, 18771−18778

morphological and compositional point of view, but the information about the interaction of the materials on the interface is scarce.

As CMOS scaling approaches its limits, devices utilizing different physical phenomena have emerged. In this sense, electrochemical metallization (ECM) cells are promising candidates for nonvolatile resistive switching random access memory (RRAM) devices.[31] ECM cells are normally formed by a functional switching material in between two electrodes. Their switching mechanism relies on an electrochemical formation of a nanometer-sized metallic filament ("SET") and an electrochemical dissolution of this filament ("RESET"). The Cu/SiO_2 system is a good choice in order to form ECM cells, and several research groups are interested not only in improving the devices[32−35] but also in understanding the formation of the nanometer-sized Cu filaments.[36−39]

Compared to the bulk properties, relatively little is known not only about the surface properties of Cu-silica mixed oxides but also about the first stages of oxidation of the Cu/SiO_2 interface. Therefore, the main objective of this work is the study of the growth kinetics of the Cu/SiO_2 interface from a chemical point of view by the use of X-ray photoelectron spectroscopy (XPS). Moreover, angle resolved X-ray photoelectron spectroscopy (ARXPS) measurements have been carried out in order to explore the morphology of the interface formed. These kind of measurements provide information at different depths, which allows us to infer the evolution of a depth profile during the Cu/SiO_2 interface formation.

EXPERIMENTAL SECTION

SiO_2 was thermally grown on p-type Si(111) wafers, obtaining an oxide film of 170 nm in thickness. This SiO_2 was used as substrate through all the experiment. The SiO_2/Si substrate was introduced into the sample preparation chamber, operating at a pressure better than 1×10^{-7} mbar. No previous cleaning process was performed on the SiO_2 substrate prior to Cu evaporation. Cu deposition was carried out by electron beam (e-beam) evaporation (Telemark TT-8 model) at room temperature, using Cu pellets (99.9995% purity) provided by Sigma-Aldrich. The e-beam was operated at 8.8 kV, and the current was varied from 16 to 18 mA in order to maintain a constant evaporation rate of 0.01 nm/s measured with a quartz microbalance (QMB). Once the Cu was evaporated, the samples were transferred to the analysis chamber without breaking the vacuum.

In the analysis chamber, XPS spectra were measured using a hemispherical analyzer (Physical Electronics 1257 system). A twin anode (Mg and Al) X-ray source was operated at a constant power of 400 W using Al Kα radiation (1486.6 eV) for the XPS measurements. The samples were placed in a sample stage in which the emission angle can be varied between 0° and 70°. Before the spectral analysis, the binding energy (BE) was calibrated with the adventitious carbon signal centered at 285.0 eV (more information in Table SI1). Also, a Shirley background subtraction[40] was applied on all the spectra. The morphology of films was characterized by scanning probe microscopy (SPM) at room temperature (SPM1 system from Omicron operating in vacuum). In AFM, the contact mode was used. The images were processed with a linear plane fit in order to remove the tilt with WSxM.[41]

RESULTS

Figure 1 shows the evolution of the Si 2p, Cu $2p_{3/2}$, Cu LMM, and O 1s photoelectron peaks measured during the Cu/SiO_2 interface formation at normal emission for different Cu depositions. Some of the spectra have been magnified for the purpose of comparison. Each spectrum is labeled by its Cu/Si concentration ratio. The intensities (band areas) of Si 2p, Cu $2p_{3/2}$, O 1s, and C 1s were used to calculate the concentration using the following eq 1

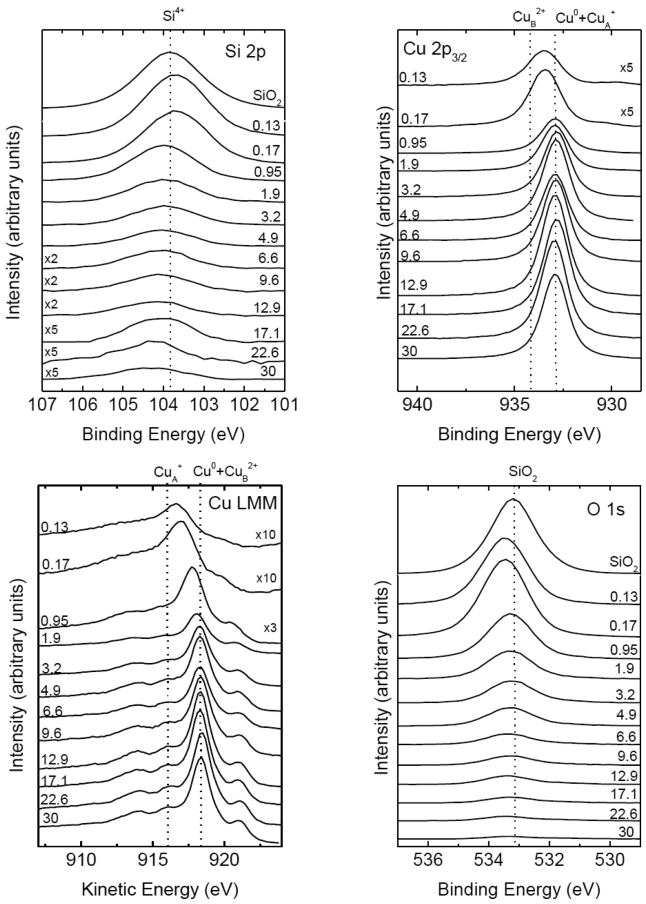

Figure 1. XPS and AES high resolution spectra of Si 2p, Cu $2p_{3/2}$, Cu LMM, and O 1s bands measured for different Cu/Si ratios during the Cu/SiO_2 interface formation. Each spectrum is labeled with the Cu/Si ratio.

$$C_x = \frac{I_x/S_x}{\sum_i I_i/S_i} \quad (1)$$

where C_x is the atomic concentration of element x, assumed to be uniform on the surface, I_x is the measured intensity for this element, and S_x is its sensitivity factor provided by the analysis software (CasaXPS).[42]

In the case of the Si 2p band (Figure 1), the SiO_2 substrate was measured as reference (dotted line). This spectrum is fitted with a unique peak centered at 103.9 eV with a full width at half-maximum fwhm = 1.85 eV. During the Cu/SiO_2 interface formation, a shift from 103.7 to 104.2 eV was observed in this band as the Cu thickness increases. This shift in the binding energy is indicative of a change in the chemical environment, the presence of a new chemical state, or differential charging between the surface Cu and the SiO_2.[26,43] Analyzing the Si 2p

DOI: 10.1021/acs.jpcc.7b06563
J. Phys. Chem. C 2017, 121, 18771−18778

band during the Cu/SiO_2 interface formation in detail, it can be seen that the contribution related to SiO_2 (Si^{4+} 103.9 ± 0.3 eV) is the only one present for the Cu/SiO_2 interface formation. The shift and the widening of this peak can be due to changes in the local atomic arrangements. It is reported that the Si 2p binding energy of SiO_2 can vary by 1.5 eV depending on the number of SiO_4 tetrahedral units present in the ring, that is to say, the Si−O−Si angle (θ).[44,45] A peak at a higher binding energy appears at larger θ. This concept is of relevance when talking about interface formation since one expects not only several oxidation states of a given element but also the modification of the chemical environment when the interface is formed. On the other hand, SiO_2 could be more charged than Cu, so the charge correction may not be enough for the Si 2p band, causing the shift.

If the Cu $2p_{3/2}$ band is analyzed as the Cu thickness increases (Figure 1), a shift toward the lower binding energy side is observed. At the lowest Cu/Si ratio, the Cu $2p_{3/2}$ band is centered at 933.5 eV. As the Cu/Si ratio increases, the band shifts toward lower values toward 932.7 eV, which corresponds to metallic Cu.[46,47] This shift means that the first monolayers of Cu atoms react with the substrate, forming chemical states different from the metallic one. As the Cu thickness is increased, metallic Cu is found at the top surface. Therefore, the Cu/SiO_2 interface is formed in two different stages: the first one in which the deposited metallic Cu changes its chemical state, and the second one in which metallic Cu can be found at the surface. During fitting the Cu $2p_{3/2}$ band, five different contributions are identified: (1) 930.3 ± 0.3 eV, (2) 932.8 ± 0.1 eV, (3) 933.4 ± 0.1 eV, (4) 934.0 ± 0.1 eV, and (5) 936.1 ± 0.1 eV (see Table 1). The main band at 932.8 eV is

Table 1. Binding Energy and fwhm for Different Oxidation States and Coordination (A = Tetrahedral and B = Octahedral) Present in Cu $2p_{3/2}$ Band and Kinetic Energy for Different Oxidation States Present in Cu LMM Band

oxidation state	Cu $2p_{3/2}$ BE (eV)	fwhm (eV)	Cu LMM KE (eV)
Cu^{+}_{B}	930.3 ± 0.3	2.2 ± 0.1	
Cu^{0}	932.8 ± 0.1	1.5 ± 0.1	918.6 ± 0.1
Cu^{+}_{A}	932.8 ± 0.1	1.5 ± 0.1	916.1 ± 0.1
Cu^{x+}	933.4 ± 0.1	1.4 ± 0.1	917.2 ± 0.1
Cu^{2+}_{B}	934.0 ± 0.1	2.2 ± 0.1	918.1 ± 0.1
Cu^{2+}_{A}	936.1 ± 0.1	2.4 ± 0.1	

connected with the formation of Cu^0 and Cu^+ with tetrahedral coordination (Cu^{+}_{A}).[47,48] These two chemical states are indistinguishable in the Cu $2p_{3/2}$ band, but they are separated ~2.0 eV in the Cu LMM, as shown below.[49] The contribution Cu^0 + Cu^{+}_{A} increases as the Cu content increases, becoming in the main component of the band for Cu/Si ratios larger than 0.95, when the Cu $2p_{3/2}$ band is centered at 932.9 eV. The other components observed are the peaks at 934.0 and 936.1 eV, which correspond to Cu^{2+} with octahedral (Cu^{2+}_{B}) and tetrahedral (Cu^{2+}_{A}) coordination, respectively.[48] The lower binding energy peak at 930.6 eV is identified as a peak related to Cu^+ with octahedral coordination (Cu^{+}_{B}).[48] Finally, the peak at 933.4 eV is not reported in the literature (Cu^{x+}). The presence of a contribution near 930.6 eV has been explained as the formation of monophase Cu-M mixed oxide in other systems such as Cu-Co or Cu-Mn or as Cu^+ in ferrites and chromites in octahedral symmetry.[48,50] The contribution at 933.4 eV can be assigned to the formation of new chemical states involving Cu−O−Si bonds present during the Cu/SiO_2 interface formation. At the lowest Cu/Si ratio, the main contribution is not the one related to the formation of Cu^0 + Cu^{+}_{A}, as could be expected. Instead, Cu^{+}_{B} and Cu^{x+} are the main contributions, reaching the highest concentrations.

The evolution of the Cu $2p_{3/2}$ components as a function of Cu/Si ratio is represented in Figure 2. Dotted lines have been

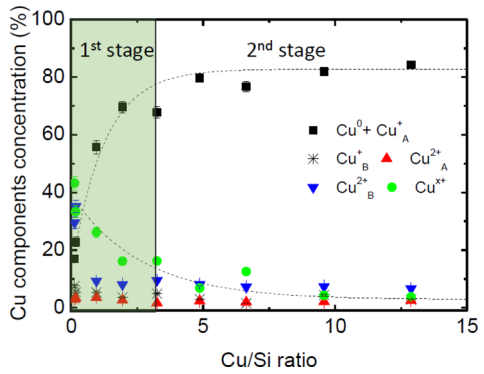

Figure 2. The concentration of Cu $2p_{3/2}$ band components as a function of the Cu/Si ratio. Dotted lines have been added to guide the eye.

added to guide the eye. Here, it can be observed that, at the beginning, the Cu^0 + Cu^{+}_{A} contribution is not the main one. This peak grows, reaching an almost stationary concentration for a Cu/Si ratio of ~3. On the other hand, Cu^{2+}_{A} and Cu^{x+} have the opposite behavior: They present their maximum concentration at the beginning of the growth process, and their concentration decreases as the Cu/Si ratio is increased. Two different stages of growth can be distinguished: the first one, where Cu reacts with the substrate, generating Cu; and the second one, where the stationary state is reached and metallic Cu is present on the surface.

Changes in the Cu can be followed better in the Cu LMM band (Figure 1). The maximum of this band appears at a kinetic energy (KE) of 916.6 eV for the lowest Cu/Si ratio, and it shifts 1.8 eV toward higher kinetic energy to 918.4 eV as more copper is deposited, a value which corresponds to metallic Cu.[49] The Cu LMM band can be used in order to identify the Cu oxidation state, providing extra information about the Cu $2p_{3/2}$ band. Cu LMM usually is fitted with one peak at a kinetic energy of 918.2 eV, which corresponds to Cu^0, another at 916.5 eV, which corresponds to Cu^{+}_{A}, and three other peaks at 913.8, 919.6, and 920.6 eV that represent different transition states of the Cu LMM.[51] In our case, during the first stage of growth, the contribution connected to Cu^0 is not present. Instead, an extra peak at 917.2 eV has to be used to fill the spectra (Table 1). This new component can be connected with the presence of the band at 933.4 eV in Cu $2p_{3/2}$, suggesting the presence of Cu−O−Si bonds in the Cu/SiO_2 interface. The spectra of the second stage of growth can be fitted using the same five peaks that are reported elsewhere,[51] being the main contribution the one present at 918.4 eV, which is the one connected to Cu^0.

The behavior of the O 1s band (Figure 1) is similar to the one observed in the Si 2p band. In this case, this band suffers a shift from 533.5 eV measured for the lower Cu/Si ratio to 533.2 eV which is the binding energy measured for the reference SiO_2 sample. If the O 1s − Si 2p separation is calculated, variations between 429.9 and 429.0 eV are observed. This shift is

DOI: 10.1021/acs.jpcc.7b06563
J. Phys. Chem. C 2017, 121, 18771−18778

indicative of changes in chemical bonding, and they are not connected with charge effects.[44] Iwata et al.[52] observed that the Si 2p and O 1s peaks shifted with the X-ray irradiation in the same direction and by the same amount when a SiO_2/Si sample is measured by XPS. This was also observed when the thickness of SiO_2 was changed. The difference between the Si 2p and O 1s peak positions is practically independent of electric charging (differences of 0.2 eV has been observed) and is considered to be a good measure of the chemical state. In our case, differences of 0.9 eV in the Si 2p − O 1s separation are due to chemical shift and not to charge effects.

Similar binding energy shifts have been previously reported. In the case of Cu $2p_{3/2}$, Greyas et al. observed a shift in the Cu $2p_{3/2}$ band after exposing a Cu/Si(100) interface to Cl_2.[53] They supposed that the shift was due to Cu dissolution onto Si(100) and/or structural changes in the near surface region of Cu/Si(100), proposing an intermix layer as the most plausible growth theory. Sarkar et al. also observed a 0.3 eV shift when a Cu/Si(100) interface is irradiated with 80 keV Ar^+ ions, which they attribute to silicide formation.[54] In our case, the binding energy shift of the signals and the presence of a new contribution in Cu $2p_{3/2}$ and Cu LMM can be interpreted as the formation of a mixed oxide Cu-O-Si in the interface.

Further information on the composition and morphology of the interface formation is obtained using ARXPS measurements. A set of spectra from each of the two stages have been chosen: (1) the first stage, where no metallic Cu is detected (Cu/Si = 0.13), and (2) the second stage, where the Cu^0 + Cu_A^+ contribution of the Cu $2p_{3/2}$ band reaches the stationary state (Cu/Si = 4.9)

Figure 3 shows ARXPS measurements of the Cu $2p_{3/2}$, Si 2p, and O 1s bands performed at the first stage of growth,

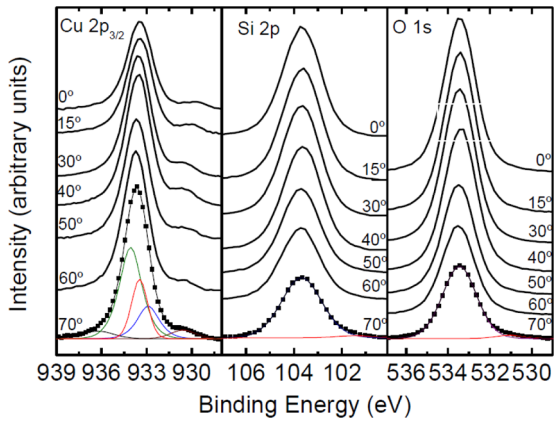

Figure 3. ARXPS measurements of the Cu $2p_{3/2}$, Si 2p, and O 1s bands performed for a Cu/Si ratio = 0.13. Each spectrum is labeled by the take-off angle.

characterized by a Cu/Si ratio around 0.1. The Si 2p band shows a main component centered at 103.8 eV for the whole set of measurements, corresponding to SiO_2. At take-off angles larger than 50°, a new contribution appears (Si^{x+}) at a lower energy (101.5 ± 0.1 eV). If the O 1s band is observed, it presents a main contribution centered at 533.4 eV which corresponds to O−Si bonds,[55] accompanied by a small peak at the low energy side (O^x at 531.2 eV). This new contribution has a binding energy higher than that expected for Cu−O bonds, so it can be associated with a new contribution. The Cu $2p_{3/2}$ band is more complex to analyze: the spectrum measured at normal incidence is centered at 933.4 eV. As the take-off angle is increased, the band shifts to the higher binding energy side, reaching 933.7 eV. Moreover, a shoulder is observed at the lower energy side. This contribution, related to Cu_B^+, shifts from 929.8 to 930.6 eV as the take-off angle increases, which indicates a modification in the chemical environment.[50] All Cu $2p_{3/2}$ spectra can be fitted by the five contributions mentioned above (see Table 1). In this case, the contribution at 932.7 eV is related only to the presence of Cu_A^+, as can be inferred looking at Cu LMM and Cu $2p_{3/2}$ bands simultaneously (see Figure 1). It can be concluded that, during the first stage of growth, oxygen from the SiO_2 substrate reacts with the deposited Cu, forming a thin layer composed by a mixture of Cu oxides and Cu-O-Si mixed oxide. Summarizing, the Si 2p band presents a component Si^{x+} at a binding energy below that of SiO_2, the Cu $2p_{3/2}$ presents components Cu^{x+} at a binding energy higher than the one of Cu^+, and the O 1s band presents a component O^x somewhere between those of SiO_2 and Cu_2O, therefore indicating that the Cu−O bonds are more ionic and the Si−O bonds are more covalent than in pure Cu_2O and SiO_2 oxides, respectively. According to Barr,[56] this behavior can be interpreted as due to the formation of a Cu-O-Si mixed oxide instead of the formation of single oxide phases.

Figure 4 shows ARXPS measurements of the Cu $2p_{3/2}$, Si 2p, and O 1s bands performed at the second stage of growth,

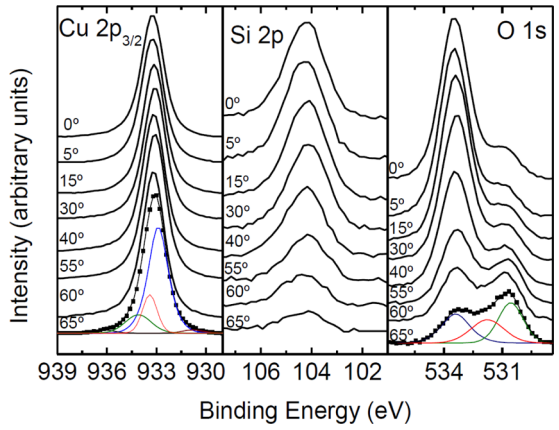

Figure 4. ARXPS measurements of the Cu $2p_{3/2}$, Si 2p, and O 1s bands performed for a Cu/Si ratio = 4.9. Each spectrum is labeled with the take-off angle.

characterized by a Cu/Si ratio around 5. If the Cu $2p_{3/2}$ band is analyzed, a small shift from 933.3 to 933.1 eV is observed as the take-off angle increases. This difference in the binding energy suggests a gradual change in the chemical composition of the film. In the case of the Si 2p peak, the narrow band measured at 0° becomes less intense and wider with increasing take-off angle. The SiO_2 signal from the substrate decreases at large take-off angle measurements (more sensitive to the surface). The widening of the band is related to changes in the Si−O−Si angle θ, as mentioned above. In the case of the O 1s band, three different contributions are needed to reproduce the whole band, as it is shown in Figure 4. The contribution at 533.5 eV is connected with the presence of SiO_2;[55] the one at 530.6 eV is related to the formation of CuO and Cu_2O.[46] A third contribution becomes necessary between those already mentioned, which shifts from 532.2 to 531.7 eV as the take-off angle is increased, to fill the whole spectra. This third contribution has been observed in other systems as Ti/Si

DOI: 10.1021/acs.jpcc.7b06563
J. Phys. Chem. C 2017, 121, 18771−18778

irradiated by O_2^+ and it is associated with the presence of a new chemical state (Ti-O-Si mixed oxide).[55] In the case of the Cu/SiO_2 system, this contribution is connected with the formation of a Cu-O-Si mixed oxide. This contribution is consistent with the presence of the contribution Cu^{x+} at 933.4 eV in the Cu $2p_{3/2}$ band and the contribution at 917.2 eV in the Cu LMM band.

DISCUSSION

It has been observed that, during the growth of the Cu/SiO_2 interface, Cu $2p_{3/2}$ and Cu LMM bands shift to lower binding and higher kinetic energies, respectively, as the Cu thickness is increased (Figure 1). The shifts in the Cu $2p_{3/2}$ and Cu LMM are also reflected in the modified Auger parameter (α' = BE + KE), which is not affected by charge effects. Morales et al.[57] observed that Cu LMM band shifts toward higher kinetic energy during the Cu_2O/SiO_2 and CuO/SiO_2 interface formation, which leads to a variation in the modified Auger parameter. This shift may be due to several causes: (1) changes in the average coordination number of the atoms owing to a high surface-to-volume ratio; (2) a decrease of the electron density with respect to the bulk metal; (3) a narrowing of the valence band; and (4) alloying and/or chemical interactions with the substrate. For a general overview, changes in BE and α' are represented in the Wagner plot in Figure 5. These plots

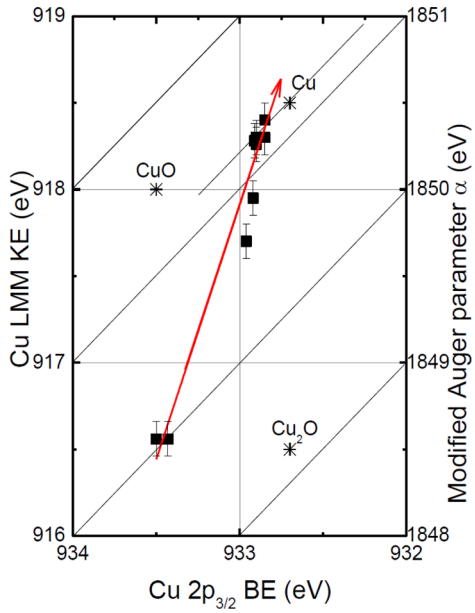

Figure 5. Wagner plot describing changes in kinetic energy (KE) and Auger parameter (α) as a function of the binding energy (BE). The arrow indicates the direction of growth of Cu/Si ratio. The asterisks mark values for reference Cu, Cu_2O, and CuO.

provide detailed information on photoelectron and Auger energies as well as the Auger parameter. On this graph, the kinetic energies of Auger electrons are on the ordinate and the binding energies of the photoelectrons are on the abscissa. Each chemical state then occupies a unique position on the two-dimensional grid. An Auger parameter grid is also drawn as a family of parallel lines with a slope of +1. All points on any one of these lines have the same value of the Auger parameter. Errors in charge referencing introduce uncertainty in data points parallel to the Auger parameter grid.[58,59]

In Figure 5, data corresponding to bulk Cu, Cu_2O, and CuO are represented by an asterisk for comparison purposes and full squares represent the measured values for increasing Cu thickness. The arrow represents the shift of the values as Cu thickness is increased. It is easy to realize that, for the lowest Cu thickness, α' has the lowest values. When the Cu thickness increases, the Auger parameter grows too, reaching α' values near the one of metallic Cu. The Auger parameter continuously grows as a function of the Cu thickness. This shift provides a direct measurement of the extra-atomic relaxation energy. Furthermore, points in the Wagner plot can be fitted by a line with slope −3, which means that only the final states are responsible for the changes in electronic parameters.[59] Changes in extra-atomic relaxation energy of the photohole in the final state, ΔRE, and in the energy of the initial state of the system, $\Delta\epsilon$, are connected with this shift, as shown in eqs 2 and 3[59]

$$\Delta \mathrm{RE} = \frac{1}{2}\Delta\alpha' = 0.6 \text{ eV} \tag{2}$$

$$\Delta\epsilon = \Delta \mathrm{BE} + \Delta \mathrm{RE} = -0.2 \text{ eV} \tag{3}$$

An increase of ΔRE means that a photoelectron has been suddenly created in an atom, which produces extra energy in the system due to the accommodation of free electrons. It is a direct measurement of a change in the local coordination around the Cu atoms. Meanwhile, ϵ describes the initial state energy of the system. A change in this parameter means an alteration in the charge density and in the Madelung potential around the atom. $\Delta\epsilon < 0$ means a decrease in the negative value of Madelung potential, which means a lower coordination number.

To determine the growth mode of Cu on SiO_2, the ratios I_0/I_s are plotted as a function of the Cu thickness, where I_0 represents the intensity of the Si 2p band for the reference sample and I_s represents the intensity of the Si 2p measured during the growth kinetics of Cu. Two theoretical models are considered: a layer-by-layer growth Frank−van der Mewer (FM) and an island growth Volmer−Weber (VW).[60] The theoretical expressions which represent the 2D and 3D growth are eqs 4 and 5, respectively

$$\text{FM: } I_s/I_0 = \exp(-d/\lambda) \tag{4}$$

$$\text{VW: } I_s/I_0 = (1-\theta) + \theta \exp(-d/\lambda) \tag{5}$$

where d is the Cu thickness measured with the QMB during the evaporation, λ is the inelastic mean free path from the Tanuma, Powell, and Penn (TPP2M) formula[61] and θ is the coverage of the islands. Figure 6 shows I_0/I_s as a function of the Cu thickness together with FM and VM growths, using λ = 2.4 nm, which is the value obtained for Cu oxide and θ = 95%.

It is possible to infer a qualitative model of the interface formation using the intensities from ARXPS measurements. Figure 7 shows the variation of $Cu_B^{2+}/(Cu^{x+} + Cu_B^{+} + Cu_A^{+} + Cu_A^{2+})$, $Cu^{x+}/(Cu_B^{+} + Cu_A^{+} + Cu_A^{2+})$, $Cu_A^{2+}/(Cu_B^{+} + Cu_A^{+})$, and Cu_B^{+}/Cu_A^{+} (some of these ratios have been magnified for the purpose of comparison), derived from Figure 3 as a function of the take-off angle for the first stage of growth. The results are consistent with the sequence indicated in the simplified model of Figure 7, that is, Cu_B^{2+}, the new contribution Cu^{x+}, Cu_A^{2+}, Cu_B^{+}, Cu_A^{+}, and the SiO_2 substrate when going from the outer surface to the substrate.

In the second stage of growth, qualitative information can be obtained from the O 1s and Cu $2p_{3/2}$ bands shown in Figure 4.

DOI: 10.1021/acs.jpcc.7b06563
J. Phys. Chem. C 2017, 121, 18771−18778

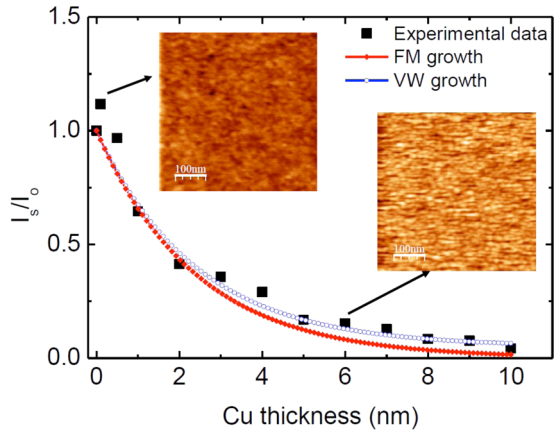

Figure 6. I_0/I_s as a function of the Cu thickness, where I_0 represents the intensity of the Si 2p band for the reference sample and I_s represents the intensity of the Si 2p measured during the growth kinetics of Cu. Red squares represent theoretical calculations for FM growth and blue circles theoretical calculations for SK growth with a surface coverage of 95%. The insets show AFM measurements for Cu thickness of 0.1 and 5 nm, respectively.

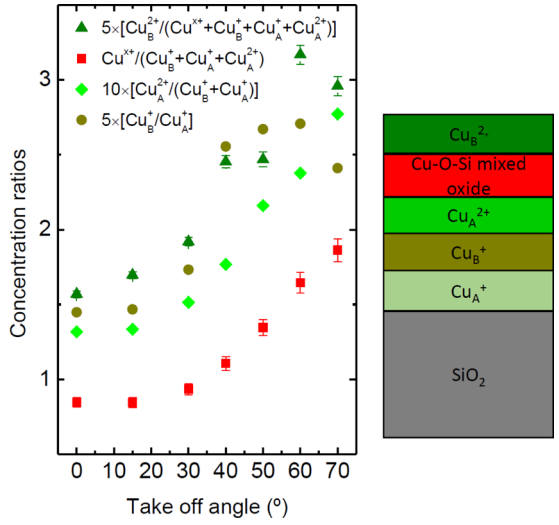

Figure 7. On the left side, the variation of the concentration ratios $Cu_B^{2+}/(Cu^{x+} + Cu_B^{+} + Cu_A^{+} + Cu_A^{2+})$, $Cu^{x+}/(Cu_B^{+} + Cu_A^{+} + Cu_A^{2+})$, $Cu_A^{2+}/(Cu_B^{+} + Cu_A^{+})$, and Cu_B^{+}/Cu_A^{+} as a function of the take-off angle inferred from Figure 3. On the right side, the growth model inferred for the first stage of growth.

In the case of the O 1s band, the ratios O-Cu-Si/O-Cu and O-Cu/O-Si grow as the take-off angle is increased (Figure 8), which evidences the presence of a mixed oxide Cu-O-Si onto the Cu oxides layer. This can be attributed to the migration of Si atoms toward the surface. This phenomenon has been observed in other similar systems.[55] In this band, it is not possible to distinguish between the different oxidation states of copper. In this sense, Cu $2p_{3/2}$ and Cu LMM bands can be used. Precise intensities of Cu^0 and Cu_A^{2+} in the Cu LMM spectrum were calculated by applying a correction factor, ϕ, which takes into account an emission probability of an Auger electron, γ, the difference in transmission functions of these two spectra, T(KE), and the difference in the photoionization cross section, σ.[62] Therefore, the Cu_A^{2+} intensity in the Cu LMM spectrum was determined by multiplying ϕ with the Cu_A^{2+} intensity obtained from the Cu $2p_{3/2}$ spectrum of the Cu film of

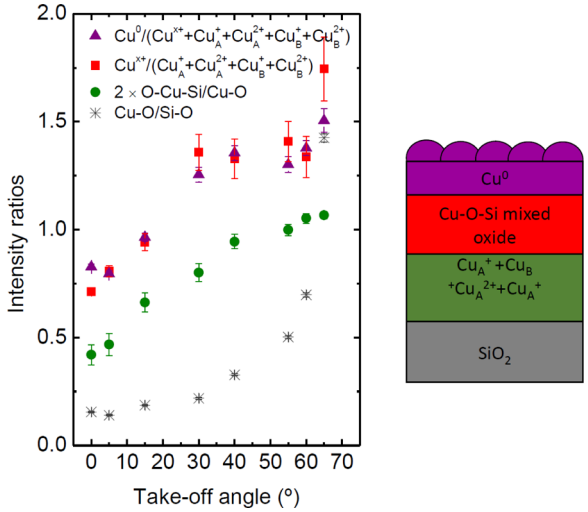

Figure 8. On the left side, the variation of the concentration ratios $Cu^0/(Cu^{x+} + Cu_B^{+} + Cu_A^{+} + Cu_A^{2+} + Cu_B^{2+})$, $Cu^{x+}/(Cu_B^{+} + Cu_A^{+} + Cu_A^{2+} + Cu_B^{2+})$, O-Cu-Si/Cu-O, and Cu-O/Si-O as a function of the take-off angle inferred from Figure 4.On the right side, the growth model inferred for the second stage of growth.

100 nm evaporated and measuring by XPS without exposing it to ambient conditions. ϕ was derived as follows:[49]

$$\phi = \frac{I_{\text{Cu metal}}(\text{Cu LMM})}{I_{\text{Cu metal}}(\text{Cu } 2p_{3/2})} \quad (6)$$

Using the information obtained by applying ϕ, Cu^0 and Cu_A^{+} intensities can be separated and a qualitative model of the interface formation using intensity can be inferred (Figure 8). If $Cu^0/(Cu_B^{2+} + Cu^{x+} + Cu_B^{+} + Cu_A^{+} + Cu_A^{2+})$ is represented as a function of the take-off angle, it can be seen that the ratio increases, which indicates that Cu^0 is on the surface. Moreover, the $Cu^{x+}/(Cu_B^{+} + Cu_A^{+} + Cu_A^{2+} + Cu_B^{2+})$ ratio is represented in Figure 7. From these ratios, a depth profile model can be inferred based on a multilayer $Cu^0/Cu^{x+}/(Cu_B^{2+} + Cu_B^{+} + Cu_A^{+} + Cu_A^{2+})$ onto the SiO_2 substrate. All of these ratios are represented in Figure 8.

CONCLUSIONS

The formation of the Cu/SiO_2 interface has been studied. During the growth kinetics, the presence of different Cu oxides is observed, with different coordination. Furthermore, a new species appears during the interface formation (Cu^{x+}) and it has been assigned to the formation of a mixed oxide Cu-O-Si.

During the Cu deposition onto SiO_2, two different stages of growth can be distinguished. The first one, where no metallic Cu is detected and a mixture of copper oxides is measured onto the SiO_2 substrate, and the second one, where metallic Cu appears on the surface and a multilayer Cu^0/Cu^{x+}/Cu oxides/SiO_2 can be inferred.

ASSOCIATED CONTENT

Supporting Information

The Supporting Information is available free of charge on the ACS Publications website at DOI: 10.1021/acs.jpcc.7b06563.

Table SI1 including initial position of C 1s band, charge correction, and Auger parameter measured during the kinetics of growth (PDF)

DOI: 10.1021/acs.jpcc.7b06563
J. Phys. Chem. C 2017, 121, 18771−18778

AUTHOR INFORMATION

Corresponding Author

*E-mail: noelia.benito@ing.uchile.cl. Phone: +56 2 29784523.

ORCID

Noelia Benito: 0000-0002-5943-8942

Author Contributions

All authors have contributed equally to the studies reported in this manuscript.

Notes

The authors declare no competing financial interest.

ACKNOWLEDGMENTS

We thank Fondo Nacional de Desarrollo Científico FONDECYT for financial support (projects 3150101 and 1140759). The authors greatly acknowledge Prof. Victor Fuenzalida for his contribution in the discussion of results.

REFERENCES

(1) Matula, R. A; Electrical Resistivity of Copper, Gold, Palladium, and Silver. *J. Phys. Chem. Ref. Data* **1979**, *8*, 1147−1298.

(2) Kendelewicz, T.; Rossi, G.; Petro, W. G.; Babalola, I. A.; Landau, I.; Spicer, W. E. Similarities in Chemical Intermixing at the Cu/lnP and Cu/Si Interfaces. *J. Vac. Sci. Technol., B: Microelectron. Process. Phenom.* **1983**, *1* (3), 564−569.

(3) McBrayer, J. D.; Swanson, R. M.; Sigmond, T. W. Diffusion of Metals in Silicon Dioxide. *J. Electrochem. Soc.* **1986**, *133*, 1242−1246.

(4) Oku, T.; Kawakami, E.; Uekubo, M.; Takahiro, K.; Yamaguchi, S.; Murakami, M. Diffusion Barrier Property of TaN Between Si and Cu. *Appl. Surf. Sci.* **1996**, *99*, 265−272.

(5) Imahori, J.; Oku, T.; Murakami, M. Diffusion Barrier Properties of TaC Between Si and Cu. *Thin Solid Films* **1997**, *301*, 142−148.

(6) Kim, D. J.; Jung, Y. B.; Lee, M. B.; Lee, Y. H.; Lee, J. H.; Lee, J. H. Applicability of ALE TiN Films as Cu/Si Diffusion Barriers. *Thin Solid Films* **2000**, *372*, 276−283.

(7) Ono, H.; Nakano, T.; Ohta, T. Diffusion Barrier Effects of Transition Metals for Cu/M/Si Multilayers (M = Cr, Ti, Nd, Ta, W). *Appl. Phys. Lett.* **1994**, *64* (12), 1511−1513.

(8) Lee, C.; Kuo, Y. L. The Evolution of Diffusion Barriers in Copper Metallization. *JOM* **2007**, *59*, 44−49.

(9) Wang, S. Q. Barriers Against Copper Diffusion into Silicon and Drift Through Silicon Dioxide. *MRS Bull.* **1994**, *19*, 30−40.

(10) Eisenbraun, E. Ultimate Limits of Conventional Barriers and Liners-Implications for the Extendibility of Copper Metallization. *Microelectron. Eng.* **2012**, *92*, 67−70.

(11) King, S. W. Dilectric Barriers, Etch Stop, and Metal Capping Materials for State of Art and Beyong Metal Interconectors. *ECS J. Solid State Sci. Technol.* **2015**, *4* (1), N3029−N3047.

(12) Park, J.-H.; Han, D.-S.; Kang, Y.-J.; Shin, S.-R.; Park, J.-W. Self-Forming Al Oxide Barrier for Nanoscale Cu Interconnects Created by Hybrid Atomic Layer Deposition of Cu−Al Alloy. *J. Vac. Sci. Technol., A* **2014**, *32*, 01A131.

(13) Byrne, C.; Brennan, B.; McCoy, A. P.; Bogan, J.; Brady, A.; Hughes, G. In Situ XPS Chemical Analysis of $MnSiO_3$ Copper Diffusion Barrier Layer Formation and Simultaneous Fabrication of Metal Oxide Semiconductor Electrical Test MOS Structures. *ACS Appl. Mater. Interfaces* **2016**, *8*, 2470−2477.

(14) Casey, P.; Bogan, J.; McCoy, A.; Lozano, J. G.; Nellist, P. D.; Hughes, G. Chemical and Structural Investigations of the Interactions of Cu with $MnSiO_3$ Diffusion Barrier Layer. *J. Appl. Phys.* **2012**, *112*, 064507.

(15) Hino, A.; Okuno, H.; Kugimiya, T. Study of Adhesion and Chemical Bonds in the Reaction Layer Formed at Cu-Mn Interconnection/SiO_2 Interface. *J. Appl. Phys.* **2013**, *113*, 174902.

(16) He, M.; Novak, S.; Vanamurthy, L.; Bakhru, H.; Plawsky, J.; Lu, T.-M. Cu Penetration into Low-k Dielectric During Deposition and Bias-Temperature Stress. *Appl. Phys. Lett.* **2010**, *97*, 252901.

(17) Cui, H.; Bhat, I. B.; Murarka, S. P.; Lu, H.; Hsia, W. J.; Catabay, W. Copper Drift in Methyl-Doped Silicon Oxide Film. *J. Vac. Sci. Technol., B: Microelectron. Process. Phenom.* **2002**, *20*, 1987−1993.

(18) Guo, X.; King, S. W.; Zheng, H.; Xue, P.; Nishi, Y.; Shohet, J. L. Effects of Vacuum-Ultraviolet Irradiation on Copper Penetration into Low-k Dielectrics under Bias-Temperature Stress. *Appl. Phys. Lett.* **2015**, *106*, 012904.

(19) Guo, X.; Pei, D.; Zheng, H.; Li, W.; Shohet, J. L.; King, S. W.; Lin, I. H.; Fung, H.-S.; Chen, C.-C.; Nishi, Y. Extrinsic Time-Dependent Dielectric Breakdown of Low-k Organosilicate Thin Films from Vacuum-Ultraviolet Irradiation. *J. Vac. Sci. Technol., A* **2017**, *35*, 021509−021509.

(20) Zhang, J.; Liu, C.; Shu, Y.; Fan, J. Growth and Properties of Cu Thin Film Deposited on Si (0 0 1) Substrate: A molecular Dynamics Simulation Study. *Appl. Surf. Sci.* **2012**, *261*, 690−696.

(21) Zhang, J.; Liu, C.; Fan, J. Comparison of Cu Thin Films Deposited on Si Substrates With Different Surfaces and Temperatures. *Appl. Surf. Sci.* **2013**, *276*, 417−423.

(22) Savchenkov, A.; Shukrinov, P.; Mutombo, P.; Slezák, J.; Cháb, V. Initial Stages of Cu/Si Interface Formation. *Surf. Sci.* **2002**, *507−510*, 889−894.

(23) Shi, J. R.; Lau, S. P.; Sun, Z.; Shi, X.; Tay, B. K.; Tan, H. S. Structural and Electrical Properties of Copper Thin Films Prepared by Filtered Cathodic Vacuum Arc Technique. *Surf. Coat. Technol.* **2001**, *138*, 250−255.

(24) Benouattas, N.; Mosser, A.; Raiser, D.; Faerber, J.; Bouabellou, A. Behaviour of Copper Atoms in Annealed Cu/SiO_x/Si Systems. *Appl. Surf. Sci.* **2000**, *153*, 79−84.

(25) Benouattas, N.; Mosser, A.; Bouabellou, A. Surface Morphology and Reaction at Cu/Si Interface—Effect of Native Silicon Suboxide. *Appl. Surf. Sci.* **2006**, *252*, 7572−7577.

(26) Espinós, J. P.; Morales, J.; Barranco, A.; Caballero, A.; Holgado, J. P.; González-Elipe, A. R. Interface Effects for Cu, CuO, and Cu_2O Deposited on SiO_2 and ZrO_2. XPS Determination of the Valence State of Copper in Cu/SiO_2 and Cu/ZrO_2 Catalysts. *J. Phys. Chem. B* **2002**, *106*, 6921−6929.

(27) Lambert, S.; Cellier, C.; Grange, P.; Pirard, J. P.; Heinrichs, B. Synthesis of Pd/SiO_2, Ag/SiO_2, and Cu/SiO_2 Cogelled Xerogel Catalysts: Study of Metal Dispersion and Catalytic Activity. *J. Catal.* **2004**, *221*, 335−346.

(28) Janas, J.; Gurgul, J.; Socha, R. P.; Dzwigaj, S. 2009, Effect of Cu Content on the Catalytic Activity of CuSiBEA Zeolite in the SCR of NO by Ethanol: Nature of the Copper Species. *Appl. Catal., B* **2009**, *91* (1), 217−224.

(29) van den Oetelaar, L. C. A.; Partridge, A.; Toussaint, S. L. G.; Flipse, C. F. J.; Brongersma, H. H. A Surface Study of Model Catalyst. 1. Quantitative Surface Analysis of Wet-Chemically Prepared Cu/SiO_2 Model Catalysts. *J. Phys. Chem. B* **1998**, *102*, 9541−9549.

(30) van den Oetelaar, L. C. A.; Partridge, A.; Stapel, P. J. A.; Flipse, C. F. J.; Brongersma, H. H. A Surface Science Study of Model Catalysts. 2. Metal−Support Interactions in Cu/SiO_2 Model Catalysts. *J. Phys. Chem. B* **1998**, *102*, 9532−9540.

(31) Waser, R.; Dittmann, R.; Staikov, G.; Szot, K. Redox-Based Resistive Switching Memories − Nanoionic Mechanisms, Prospects, and Challenges. *Adv. Mater.* **2009**, *21*, 2632−2663.

(32) Schindler, C.; Staikov, G.; Waser, R. Electrode Kinetics of Cu−SiO_2-Based Resistive Switching Cells: Overcoming. *Appl. Phys. Lett.* **2009**, *94*, 072109−072111.

(33) Bernard, Y.; Renard, V. T.; Gonon, P.; Jousseaume, V. Back-End-of-Line Compatible Conductive Bridging RAM Based on Cu and SiO_2. *Microelectron. Eng.* **2011**, *88*, 814−816.

(34) Liu, C. Y.; Huang, Y. H.; Ho, J. Y.; Huang, C. C. Retention Mechanism of Cu-Doped SiO_2-Based Resistive memory. *J. Phys. D: Appl. Phys.* **2011**, *44*, 205103−205106.

(35) Nandakumar, S. R.; Minvielle, M.; Nagar, S.; Dubourdieu, C.; Rajendran, B. A 250 mV Cu/SiO_2/W Memristor with Half-Integer Quantum Conductance States. *Nano Lett.* **2016**, *16*, 1602−1608.

DOI: 10.1021/acs.jpcc.7b06563
J. Phys. Chem. C 2017, 121, 18771−18778

(36) Cho, D. Y.; Tappertzhofen, S.; Waser, R.; Valov, I. Bond Nature of Active Metalions in SiO_2-Based Electrochemical Metallizations Memory Cells. *Nanoscale* **2013**, *5*, 1781−1784.
(37) Li, C.; Jiang, H.; Xia, Q. Low Voltage Resistive Switching Devices Based on Chemically Produced Silicon Oxide. *Appl. Phys. Lett.* **2013**, *103*, 062104.
(38) Guzman, D. M.; Onofrio, N.; Strachan, A. Stability and Migration of Small Copper Clusters in Amorphous Dielectrics. *J. Appl. Phys.* **2015**, *117*, 195702.
(39) Onofrio, N.; Guzman, D.; Strachan, A. Atomic Origin of Ultrafast Resistance Switching in Nanoscale Electrometallization Cells. *Nat. Mater.* **2015**, *14*, 440−446.
(40) Shirley, D. A. High-Resolution X-Ray Photoemission Spectrum of the Valence Band Gold. *Phys. Rev. B: Condens. Matter Mater. Phys.* **1972**, *5*, 4709−4714.
(41) Horcas, I.; Fernández, R.; Gómez-Rodríguez, J. M.; Colchero, J.; Gómez-Herrero, J.; Baro, A. M. WSXM: A Software for Scanning Probe Microscopy and a Tool for Nanotechnology. *Rev. Sci. Instrum.* **2007**, *78*, 013705.
(42) *CasaXPS v2.0 User's Manual*; Casa Software Ltd.: Devon, U.K., 2001. www.casaxps.com.
(43) Bersch, E.; Di, M.; Consiglio, S.; Clark, R. D.; Leusink, G. J.; Diebold, A. C. Complete band offset characterization of the HfO_2/SiO_2/Si stack using charge corrected x-ray photoelectron spectroscopy. *J. Appl. Phys.* **2010**, *107*, 043702.
(44) Grunthaner, F. J.; Grunthaner, P- J.; Vasquez, R. P.; Lewis, B. F.; Maserjian, J.; Madhukar, A. High-Resolution X-Ray Photoelectron Spectroscopy as a Probe of Local Atomic Structure: Application to Amorphous SiO_2 and the Si-SiO_2 Interface. *Phys. Rev. Lett.* **1979**, *43* (22), 1683−1686.
(45) Grunthaner, F. J.; Lewis, B. F.; Zamini, N.; Maserjian, J.; Madhukar, A. Chemical and Electronic Structure of the SiO_2/Si Interface. *IEEE Trans. Nucl. Sci.* **1980**, *27* (6), 1640−1646.
(46) Zuo, Z. J.; Li, J.; Han, P. D.; Huang, W. XPS and DFT Studies on the Autoxidation Process of Cu Sheet at Room Temperature. *J. Phys. Chem. C* **2014**, *118*, 20332−20345.
(47) Saikova, S.; Vorobyev, S.; Likhatski, M.; Romanchenko, A.; Erenburg, S.; Trubina, S.; Mikhlin, Y. X-Ray Photoelectron, Cu L3MM Auger and X-ray Absorption Spectroscopic Studies of Cu Nanoparticles Produced in Aqueous Solutions: The Effect of Sample Preparation Techniques. *Appl. Surf. Sci.* **2012**, *258*, 8214−8221.
(48) Kester, E.; Gillot, B.; Perriat, P.; Dufour, Ph.; Villette, C.; Tailhades, Ph.; Rousset, A. Thermal Behavior and Cation Distribution of Submicron Copper Ferrite Spinels $Cu_xFe_{3-x}O_4$ ($0 \leq x \leq 0.5$) Studied by DTG, FTIR, and XPS. *J. Solid State Chem.* **1996**, *126*, 7−14.
(49) Platzman, I.; Brener, R.; Haick, H.; Tannenbaum, R. Oxidation of Polycrystalline Copper Thin Films at Ambient Conditions. *J. Phys. Chem. C* **2008**, *112*, 1101−1108.
(50) la Rosa-Toro, A.; Berenguer, R.; Quijada, C.; Montilla, F.; Morallón, E.; Vazquez, J. L. Preparation and Characterization of Copper-Doped Cobalt Oxide Electrodes. *J. Phys. Chem. B* **2006**, *110*, 24021−24029.
(51) Dubot, P.; Jousset, D.; Pinet, V.; Pellerin, F.; Langeron, J. P. Simulation of the LMM Auger Spectra of Copper. *Surf. Interface Anal.* **1988**, *12*, 99−104.
(52) Iwata, S.; Ishizaka, A. Electron Spectroscopic Analysis of the SiO_2/Si System and Correlation with Metal−Oxide−Semiconductor Device Characteristics. *J. Appl. Phys.* **1996**, *79*, 6653−6713.
(53) Gheyas, S. I.; Strable, B. L.; Strongin, D. R.; Wright, A. P. Cl_2 Surface Chemistry on Cu/Si (1 0 0): an ISS, XPS, and TPD Study. *Surf. Sci.* **2001**, *474*, 129−138.
(54) Sarkar, D. K.; Bera, S.; Narasimhan, S. V.; Chowdhury, S.; Gupta, A.; Nair, K. G. M. GIXRD and XPS Investigation of Silicidation in Ion Beam Mixed CuSi(1 1 1) System. *Solid State Commun.* **1998**, *107* (8), 413−416.
(55) Benito, N.; Palacio, C. Mixed Ti−O−Si Oxide Films Formation by Oxidation of Titanium−Silicon Interfaces. *Appl. Surf. Sci.* **2014**, *301*, 436−441.
(56) Barr, T. L. Recent Advances in X-Ray Photoelectron Spectroscopy Studies of Oxides. *J. Vac. Sci. Technol., A* **1991**, *9*, 1793−1805.
(57) Morales, J.; Espinós, J. P.; Caballero, A.; Gonzalez-Elipe, A. R.; Mejias, J. A. XPS Study of Interface and Ligand Effects in Supported Cu_2O and CuO Nanometric Particles. *J. Phys. Chem. B* **2005**, *109*, 7758−7765.
(58) Wagner, C. D.; Gale, L. H.; Raymond, R. H. Two-Dimensional Chemical State Plots: A Standardized Data Set for Use in Identifying Chemical States by X-Ray Photoelectron Spectroscopy. *Anal. Chem.* **1979**, *51* (4), 466−482.
(59) Moretti, G. Auger Parameter and Wagner Plot in the Characterization of Chemical States by X-Ray Photoelectron Spectroscopy: a Review. *J. Electron Spectrosc. Relat. Phenom.* **1998**, *95*, 95−114.
(60) King, S. W.; Carlson, E. P.; Therrien, R. J.; Christman, J. A.; Nemanich, R. J.; Davis, R. F. X-ray Photoelectron Spectroscopy Analysis of GaN/(0001)AlN and AlN/(0001)GaN Growth Mechanisms. *J. Appl. Phys.* **1999**, *86* (10), 5584−5593.
(61) Tanuma, S.; Powell, C. J.; Penn, D. R. Calculations of Electron Inelastic Mean Free Paths. V. Data for 14 Organic Compounds Over the 50−2000 eV Range. *Surf. Interface Anal.* **1994**, *21*, 165−176.
(62) Tanaka, A.; Nakamura, T.; Hirokawa, K. Experimentally Derived Auger Transition Probabilities in X-Ray Excited Auger Electron Spectroscopy (XAES). *Appl. Surf. Sci.* **2001**, *169−170*, 160−163.

DOI: 10.1021/acs.jpcc.7b06563
J. Phys. Chem. C 2017, 121, 18771−18778